Uricase-deficient rat is generated with CRISPR/Cas9 technique

Yu Yun[1#], Nan Zhang[1#], Xianxiang Dong[1#], Nan Fan[1], Lei Wang[1], Yuhui Xu[1], Huan Chen[2], Weigang Duan[1,2*]

1 The Department of Pharmacology, School of Basic Medicine, Kunming Medical University, Kunming 650500, China

2 Yunnan Provincial Key laboratory of Molecular Biology for Sinomedicine, School of Basic Medicine, Yunnan University of Traditional Chinese Medicine, Kunming 650500, China

#, contributed equally to this work.

Yu Yun: yunyu_li@126.com ; ORCID: 0000-0002-0030-2194

Nan Zhang: 1016117739@qq.com ; ORCID: 0000-0002-1825-8929

Xianxiang Dong: 1737346950@qq.com ; ORCID: 0000-0003-2554-5704

Nan Fan: 3324507727@qq.com;

Lei Wang: 7176@163.com

Yuhui Xu: 562431311@qq.com

Huan Chen: qingxing1214@163.com

Corresponding author:

Corresponding author: Weigang Duan*

Mailing address: Yunnan University of Traditional Chinese Medicine, 1076, Yuhua Rd., Kunming 650500, China

Tel.: +86-86-65919552; Fax: +86-86-65918014

Mobile phone: 18687106921

E-mail: deardwg@126.com ; ORCID: 0000-0002-9006-861X

Abstract

Urate oxidase (uricase, Uox) is a big obstacle for scientists to establish stable animal models for studying hyperuricemia and associated disorders. Due to the low survival rate of uricase-deficient mice, we generated a Uox-knockout model animal from Sprague Dawley (SD) rats using the CRISPR/Cas9 technique by deleting exons 2 to 4 of the Uox gene. The uricase-deficient rats were named "Kunming-DY rats", and were apparently healthy with more than a 95% survival up to one year. The male rats' serum uric acid (SUA) increased to 48.3 ± 19.1 μg/ml, significantly higher than those of wild-type rats. Some indexes of the blood fat like total triglyceride, low density lipoprotein, and renal function indexes including blood urea nitrogen and serum creatinine were significantly different from those of wild-type rats, however, all the indexes were close to or in normal ranges. Histological renal changes including mild glomerular / tubular lesions were observed in these uricase-deficient rats. Thus, "Kunming-DY rats" with stable uricase-deficiency were successfully established and are an alternative model animal to study hyperuricemia and associated diseases mimicking human conditions.

Key words: uricase-deficiency; CRISPR/Cas9 technique; hyperuricemia; high throughput sequencing; model animal; renal function; lipid metabolism

45 **Introduction**

46   In recent decades, hyperuricemia and associated diseases have become common in modern society.

47 Hyperuricemia is a well-known disorder of purine metabolism, and the disorder can be diagnosed by having a

48 serum uric acid (SUA) above 70 μg/ ml in men or above 60 μg/ ml in women (Engel et al. 2017; Schlesinger

49 2017). The increase of SUA is caused either by uric acid over-synthesis, or by its insufficient excretion. Uric

50 acid, as an end product from purines, is directly catalyzed by xanthine dehydrogenase (Xdh) in uricase-(urate

51 oxidase, Uox) deficient creatures including humans. Uric acid and its salts are polar compounds but with poor

52 solubility (Iwata et al. 1989). The redundant uric acid and its salts are precipitated in the kidneys, bones and

53 joints as tophi, usually resulting in renal dysfunction and gout (Feig 2014); however, the relationship between

54 hyperuricemia and other diseases is still unclear (Borghi et al. 2019).

55   Uric acid can be further transformed by uricase and other enzymes to more soluble chemicals (Ramazzina

56 et al. 2006). The transformation prevents uric acid from precipitation in body fluids. However, Uox is a

57 pseudo-gene in humans, and other mammals like apes, elephants and manatees (Sharma & Hiller 2019), and

58 the gene in them cannot be translated to uricase (Keebaugh & Thomas 2010). Therefore, the deficiency of

59 uricase makes humans vulnerable to hyperuricemia and relevant diseases though it is believed to be important

60 for human evolution (Alvarez-Lario & Macarron-Vicente 2010).

61   As for researching hyperuricemia and for evaluating uric-acid-lowering drugs, naturally uricase-deficient

62 mammals could be ideal experimental animals. However, they are not commonly used in laboratories by

63 scientists. Instead, scientists use rats or mice for the convenience of breeding. Since rats and mice express

64 uricase, a uricase inhibitor, potassium oxonate was usually applied to mimic human's purine metabolism

65 (Mangoff & Milner 1978; Stavric & Nera 1978). Nevertheless, the extra inhibitor has multiple activities, which

66 would make the animal model tangled with multiple factors (Stavric & Nera 1978). To overcome the

67 shortcomings mentioned above, scientists knocked out or modified mice's Uox gene by homologous

68 recombination in embryonic stem cells (Wu et al. 1994), or by using the transcription activator-like effector

69 nuclease (TALEN) technique (Lu et al. 2018) to successfully breed heterozygote mice. However, it is still

70 difficult for scientists to breed apparently healthy homozygote animals to mimic the human condition. The

71 homozygote mice would die by 11 weeks after birth because of renal failure (Wu et al. 1994), or displayed a

72 low survival rate even kept in sterile environments (Lu et al. 2018). These findings suggested that it is a big

73 challenge to breed artificial uricase-deficient (Uox$^{-/-}$) animals. Considering that most naturally uricase-deficient

74 animals are healthy, or at least apparently healthy, the biological features of the uricase-deficient mice could be

75 deviated from humans to some extent.

76   Consequently, the knock-out or gene-modified mice left researchers with a limited choice for a model

77 animal to study hyperuricemia. However, rat is another common experimental animal, whose Uox gene has not

78 knocked out or modified. Here, to establish an alternative model animal, we tried to generate healthy uricase-

79 deficient rats, called "Kunming-DY rats", with the CRISPR/Cas9 technique.

80

Materials and methods

Materials

83   Wild-type Sprague Dawley (SD) rats were obtained from Jianyang Dashuo Science and Technology Ltd.,

84 Chengdu, China [Certification No. SCXK (Chuan) 2008–24]. Rats were maintained at 22 °C, with a humidity

85 of 45%-55% under natural light and with free approach to food and water. All animal experiments were

86 approved by Animal Care and Use Committee of Yunnan Provicial Key Laboratory of Molecular Biology for

87 Sinomedicine (Approved No. LL-20170930-01), Yunnan University of Traditional Chinese Medicine. All the

88 animal experiments were performed in accordance with Guidelines for Ethical Review of Laboratory Animal

89 Welfare of China.

90   Uric acid was purchased from Tokyo Into Industrial Co., Ltd. (Tokyo, Japan). Standard solution of uric

91 acid (1000 μg/ml, 5952 μmol/l), uric acid assay kits of phosphotungstic acid method (Lot: C012-1-1), blood

92 urea nitrogen (BUN) assay kits of diacetyl monoxime method (Lot: C013-1-1), serum creatinine (Cr) of

93 sarcosine oxidase method (Lot: C011-2-1), and protein assay kits of BCA (bicinchoninic acid) method (Lot:

94 A045-4-2) were purchased from Nanjing Jiancheng Bioengineering Institute (Nanjing, China). Total

95 triglyceride (TG) assay kits of glycerol lipase oxidase (GPO-PAP) method (Lot: A110-1-1), total cholesterol

96 (TC) assay kits of GPO-PAP method (Lot: A111-1-1), low-density lipoprotein (LDL) assay kits (Lot: A113-1-

97 1), high-density lipoprotein (HDL) assay kits (Lot: A112-1-1), and serum glucose kits of glucose oxidase

98   method (Lot: F006-1-1) were also purchased from Nanjing Jiancheng Bioengineering Institute (Nanjing,

99   China). TRIzol Plus RNA Purification kit was purchased from Introgen (Carlsbad, CA, USA). Rabbit anti-

100 mouse Uox (Lot: bs-6716R) and mouse anti-β-actin (Lot: bsm-33036M) were purchased from Beijing Bioss

101 Antibodies (Beijing, China). Goat anti- rabbit antibody linked with HRP (Lot: BA1055) and goat anti-mouse

102 antibody linked with HRP (Lot: BA1051) were purchased from Boster Biological Engineering Co., Ltd

103 (Wuhan, China). Enhanced chemoluminescence (ECL) detection kits (Lot: 34059) were purchased from Pierce

104 Biotechnology Inc (Rockford, IL, USA).

105   Ultra-pure water was produced with a Milli Q water purification system manufactured by EMD Millipore

106 Group (Darmstadt, Germany). The NanoDrop ND-1000 spectrophotometer used for experiments was

107 manufactured by PeqLab (Erlangen, Germany). The multimicroplate reader of Infinite 200pro used was

108 manufactured by Tecan Group (Mannedorf, Switzerland). A fluorescence microscope was manufactured by

109 Olympus Corp. (Tokyo, Japan). Other instruments or reagents used in the present study were made in China if

110 not mentioned.

111 **Design and generation of Uox$^{+/-}$ rat**

112   The CRISPR/Cas9 technical design and operation of generation of Uox$^{+/-}$ SD rat were pre-formed by

113 Cyagen Bioscience Inc. (www.cyagen.com). Briefly, the Uox gene is located on chromosome 2

114 (NM_053768.2; Ensembl: ENSRNOG00000016339) with 8 exons. Eight exons have been identified, with the

115 ATG start codon in Exon 1 and TGA stop codon in Exon 8. Three exons (Exon 2 to Exon 4) were selected as

116 target sites. The two pairs of gRNA targeting vectors were constructed and confirmed by sequencing. Cas9

117 mRNA and gRNA generated by in vitro transcription were co-injected into fertilized eggs for deficient rat

118 production. The pups were genotyped by PCR followed by sequence analysis. The gRNA1 (matches forward

119 strand of gene) was CCACTAGGCTAGGCGTAGCAAGG, and gRNA2 (matches reverse strand of gene) was

120 TTTTCATATTGACTGACGGCAGG.   The   links   of   gRNA   on   VectorBuilder   can   be   found   at

121 https://www.vectorbuilder.com/vector/VB171130-1198hbq.html   (gRNA1)   and

122 https://www.vectorbuilder.com/vector/VB171130-1199dvz.html (gRNA2). The target region of rat Uox locus

123 was amplified by PCR with specific primers. PCR product was sequenced to confirm targeting. The primer

124 sequence   was   GAGGTGGAGATGATTTATGCTCAGAGAC   (forward)   and

125   GAGGTCTGTGCGTCTCTCCTCATC (reverse). The PCR product was expected to be 6445 bp in wild-type

126   allele and ~600 bp in mutant allele, suggesting ~6840 bp would be deleted.

127   **Generation of Uox$^{-/-}$ rat**

128   Uox$^{+/-}$ rats were generated and identified by Cyagen Bioscience Inc. They were housed in a SPF (specific

129   pathogen free) environment, maintained at 22˚C temperature, at 45%–55% humidity-controlled conditions, and

130   under a 12-hour light-dark cycle with free access to irradiated rodent diet and sterile water. The male and

131   female animals of heterozygote (Uox$^{+/-}$) were matched to generate Uox$^{-/-}$ offspring. Likely Uox$^{-/-}$ offspring

132   were screened by their SUA level at the first round. The likely Uox$^{-/-}$male and female rats from the same

133   parental rats were also mated to generate stable Uox$^{-/-}$ offspring. When their offspring grew up, the parental

134   likely Uox$^{-/-}$ rats were further identified by their enzyme activity, protein expression, and mRNA expression.

135   The phenotype and molecular biological identification were taken until stable Uox$^{-/-}$ rats were obtained. The

136   Uox$^{-/-}$ rats of the second to the sixth generation (F2 to F6) were used to investigate their biological features

137   including body weight, SUA, BUN, Cr, and serum glucose.

138   **Blood and organ sampling**

139   Rats were kept in a small cage, and their blood sample of 0.5 ml was drawn from their tail with a tiny

140   needle without anesthetization at a local atmosphere of 28˚C-32˚C. Serum was obtained by spinning at

141   3,000× g and at 4℃ for 5 min. Serum was used for valuating uricase activity, SUA, BUN, Cr, blood fat or

142   serum glucose.

143   In order to obtain tissue samples, rats were intraperitoneally anaesthetized with urethane (1.0 g/kg). Their

144   abdomens were opened, and their livers and kidneys were harvested. Their livers were homogenated to extract

145   mRNA for RT-PCR and evaluate tissue uricase activity. Their left kidneys were used for evaluating the left

146   kidney index and used for RNA extraction, and their right kidneys were used for histological examination. The

147   left kidney was weighted and the left kidney index (LKI) was calculated by Formula-1.

148        $$Left\ Kidney\ Index\ (LKI) = \frac{weight_{left\ kidney}}{weight_{body}}\ (Formula\text{-}1)$$

149   Except rats for breeding, other rats at the conclusion of the experiment were intraperitoneally anesthetized

150   with urethane (1.0 g/kg), and their necks were dislocated for euthanasia.

151   **Uricase activity assay**

152   The maximum absorption wavelength of uric acid in weakly alkaline solution is 292 nm, and the

153   absorbance at the wavelength (A292) can be used to evaluate the level of uric acid in the solution. Enough uric

154   acid powder was dissolved in 50 mmol/l NaHCO$_3$ solution to make a uric acid saturated solution (about 1500

155   μg/ml, 20℃), and the supernatant of the solution was transferred to another tube and diluted with 50 mmol/l

156   NaHCO$_3$ to adjust its A292 (Ma et al. 2018) of a 95 μl solution in a 96-well plate from 1.5 to 2.0 (namely, 95

157   μl uric acid solution of 45-50 μg/ml). Five microliters of serum was added to 95 μl of uric acid solution and

158   mixed at 37 ˚C. An A292 of the mixture was read at an interval of 5 min for 240 min. By subtracting the A292

159   value caused by serum and the naturally degraded uric acid in a 50 mmol/l NaHCO$_3$ solution, the net A292

160   decrease (△A292) was used to evaluate uricase activity. Serum of wild-type rats contains uricase, Xdh,

161   xanthine and uric acid. At the beginning of the reaction, A292 was transiently increased in the reaction system

162   containing wild-type rat serum. The increase of A292 may have resulted from uric acid synthesis caused by

163   Xdh.

164   Similarly, liver tissue from rats was homogenated on ice, and the supernatant was obtained by spinning at

165   3,000× g and at 4℃ for 5 min. The supernatant was diluted, and the uricase activity was assayed in the same

166   reaction system as mentioned above.

167   **Western blot**

168   Rat liver tissue (about 100 mg) was homogenated in icy isotonic lysis buffer (25 mmol/l Tris, pH 7.4, 150

169   mmol/l NaCl, complete protease inhibitors from Roche (Complete, EDTA-free, glass vials, Lot: 11873580001,

170   1 mmol/l sodium orthovanadate, 1 mmol/l sodium pyrophosphate, 10 mmol/l β-glycerophosphate). The protein

171   supernatant for Western blot was obtained by spinning the homogenate at 5,000× g and at 4˚C for 5 min.

172   Protein in the supernatant was determined by the protein assay kit of BAC method. The protocol of Western

173   blot was described previously (Yun et al. 2017). Briefly, protein (50.0 μg) was applied on to 10% sodium

174   dodecyl sulfate-polyacrylamide gel electrophoresis (SDS-PAGE) and the protein was separated by a direct

175   current at 100 V. The protein in the SDS-PAGE was transferred to a nitrocellulose (NC) membrane by a direct

176   current at 10 V for 60 min in a semi-dry electrophoretic transfer cell. The NC membrane was blocked with 3%

177   bovine serum albumin at an ambient temperature for 2 hr and bathed in the primary antibody solution (1:400)

178   at 4°C overnight. The membrane was rinsed with TST Buffer (20 mmol/l Tris-HCl, pH 7.5, 0.05% Tween-20)

179   for 10 min three times, and bathed in a solution of goat anti-rabbit antibody linked with HRP (1:800) for Uox

180   detection or in a solution of goat anti-mouse antibody linked with HRP (1:800) for β-actin detection for

181   another 2 hr. The NC membrane was rinsed with TST buffer for 10 min three times and developed by the ECL

182   detection kits. The band brightness was quantified with ImageJ 1.48v software. Uricase protein from wild-type

183   rat is about 35 kDa, and β-actin protein is about 42 kDa.

184   **RT-PCR and high throughput sequencing**

185   Rat liver and kidney (about 100 mg) were frozen with liquid nitrogen and ground to powder. The total

186   RNA in the powder was extracted and purified with a TRIzol Plus RNA Purification kit. The RNA quantity

187   and quality were measured by a NanoDrop ND-1000 spectrophotometer. RNA integrity was assessed by

188   standard denaturing agarose gel electrophoresis (denatured by 0.8% methanal), and three bands in one lane

189   suggested its integrity (Chen et al. 2017; Yin et al. 2015).

190   Double-stranded cDNA (ds-cDNA) from liver was synthesized from an aliquot of total RNA using an

191   Invitrogen SuperScript ds-cDNA synthesis kit in the presence of 100 pmol/l oligo dT primers. The ds-cDNA

192   of Uox was amplified with a pair of primers: 5`-CCCATTACCATGACGACTATGG-3`(forward) and 5`-

193   GGACCTCCCATCATTCACTCTG-3`(reverse), and that of glyceraldehyde 3 phosphate dehydrogenase

194   (GAPDH, NM_017008.4) was amplified with another pair of primers: 5`-TGTGAACGGATTTGGCCGTA-

195   3`(forward) and 5`-TGAACTTGCCGTGGGTAGAG-3`(reverse). Briefly, a template (ds-cDNA) of 1 μl,

196   primers of 2 nmole and the Taq mixture (Sangon Biotech, Shanghai, China; Lot: B110006) were mixed

197   together to 50 μl. The solution of 50 μl was incubated in a PCR machine (Life Express Gradient, Hangzhou

198   Bioer Technology Co., Ltd., Hangzhou, China) 94°C for 60 s, 55°C for 60 s, 72°C for 90 s, 30 cycles, and

199   finally kept at 72°C for 20 min. The Uox product of PCR from wild-type rats is about 500 bp (462 bp), and

200   that from Uox$^{-/-}$ rat should be much shorter or not exist. GAPDH was used as control, and its product of PCR is

201   149 bp.

202   Another aliquot of total RNA from liver was sequenced with the second generation of high throughput

203   sequencing technique by Sangon Biotech (Shanghai, China). Fragments of 150 nt from Uox mRNA in liver

204   tissue were obtained by high throughput sequencing. The raw data in fastq (fq) format was transformed to

205   original sequences in fasta (fa) format by Seqkit software in a DOS (disc operation system) model (Shen et al.

206   2016). Sequences matching 27 bp or more of Uox mRNA (NM_053768) were screened out by TBtools

207   software (v0.664445552) in "Auto Blast Several Sequences To a Big File" model. By using the reference Uox

208   mRNA as a template, matched sequences were used to restore the original mRNA of Uox$^{-/-}$ rat (Conesa et al.

209   2016).

210   Total RNA from rat kidney was also sequenced with the second generation of high throughput sequencing

211   technique by Sangon Biotech. Expected values of fragment per kilobases of exon model per million mapped

212   reads (FPKM) were calculated from mapped reads, and were used for normalization of gene expression level

213   (Lin et al. 2017; Trapnell et al. 2010). Values of FPKM were used to evaluate the level of gene expression

214   associated with urate excretion or reclamation in kidney.

215   **SUA, BUN, Cr, blood fat and serum glucose determination**

216   Blood samples were drawn from tails as mentioned above. When the blood coagulated, serum was

217   obtained by spinning at $1,000\times$g for 10 min. The SUA (μg/ml) was determined with uric acid assay kits

218   according to the protocol provided by the producer. BUN (mmol/l) and Cr (nmol/l) in the serum samples were

219   determined with urea assay kits and creatinine assay kits according to the protocols provided by the producer,

220   respectively. Blood fat indexes including TG, TC, LDL, and HDL in serum and serum glucose were

221   determined with assay kits according to the protocols provided by the manufacturer. All the protocols can be

222   seen or downloaded from websites: http://www.njjcbio.com/uploadfile/product/big/20190612093216738.pdf

223   for uric acid assay; http://www.njjcbio.com/uploadfile/product/big/20190612093249433.pdf for BUN assay;

224   http://www.njjcbio.com/uploadfile/product/big/20190612093006383.pdf   for   Cr   assay;

225   http://www.njjcbio.com/uploadfile/product/big/20190611151410510.pdf   for   TG   assay;

226   http://www.njjcbio.com/uploadfile/product/big/20190611151511722.pdf   for   TC   assay;

227   http://www.njjcbio.com/uploadfile/product/big/20190611151926041.pdf   for   LDL   assay;

228   http://www.njjcbio.com/uploadfile/product/big/20190611151745050.pdf   for   HDL   assay;   and

229   http://www.njjcbio.com/products.asp?id=812 for glucose assay.

230   **Histological examination of kidney sections**

231   Rats' right kidneys were immersed in 4% paraformaldehyde solution until a routine Hematoxylin-eosin

232   (HE) staining was conducted. Paraffin-embedded sections (5 μm) of the organs were cut. The sections were

233   stained with an HE staining kit (Boster Biological Engineering Co., Ltd Wuhan, China). Images covered renal

234   cortex or medulla were visualized with the fluorescence microscope in a light mode. The scoring systems used

235   were defined as follows: glomerular abnormality: 0, normal glomeruli; 1, rare single abnormal glomerulum; 2,

236   several clusters of abnormal glomeruli; 3, massive abnormality; tubular atrophy: 0, normal tubules; 1, rare

237   single atrophic tubule; 2, several clusters of atrophic tubules; 3, massive atrophy; tubular necrosis: 0, normal

238   tubules; 1, rare single necrotic tubule; 2, several clusters of necrotic tubules; 3, massive necrosis; lymphocytic

239   infiltrates: 0, absent; 1, few scattered cells; 2, groups of lymphocytes; 3, widespread infiltrate; interstitial

240   fibrosis: 0, absent; 1, minimal fibrosis, with slight thickening of the tubular basal membrane; 2, moderate

241   fibrosis, with focal enlargement of the interstitium; 3, severe fibrosis, with confluent fibrotic areas (Debelle et

242   al. 2002).

243   **Statistical analyses**

244   Values were expressed as mean ± SD (standard deviation). If normal distribution of values was verified

245   by normality test (Shapiro-Wilk test), independent Student's t test (two-tailed) was performed to compare

246   means between groups. Otherwise, nonparametric test for two independent samples in Mann-Whitney U model

247   (two tailed) was performed. Statistical significance was accepted at $P < 0.05$.

248

249   # Results

250   **Generation of Uox$^{+/-}$ rat**

251   The CRISPR/Cas9 experiment took four rounds to generate Uox$^{+/-}$ rats. In the first two rounds,

252   CRISPR/Cas9 operation was performed successfully, but no Uox$^{+/-}$ rats were generated, possibly because of

253   off-target. In the third and fourth rounds, CRISPR/Cas9 experiments were improved, and 6 Uox$^{+/-}$ rats

254   including three female and three male rats were generated. The Uox$^{+/-}$ rats were identified with gene

255   sequencing by Cyagen Biosciences Inc. Uox$^{+/-}$ rats were apparently healthy, and no abnormal phenomenon

256   was observed. When they were 2 months old, their SUA was determined (Table 1).

257

258   **First generation of Uox$^{-/-}$ rat**

259   When Uox$^{+/-}$ rats were 2 months old, a female and a male Uox$^{+/-}$ rats from the same round were matched

260   and kept in one cage to generate Uox$^{-/-}$ offspring. About 3 weeks or more after they mated, their offspring were

261   born. The likely Uox$^{-/-}$ offspring were screened by the level of SUA 45 days after birth, or identified after their

262   natural death (if happened). In our experimental system, the SUA in adult male rats of the heterozygote type is

263   less than 20 μg/ml (Table 1), and not higher than 40 μg/ml (male) or 30 μg/ml (female). Therefore, male rats

264   with an SUA above 40 μg/ml or female rats with SUA above 30 μg/ml were recognized as likely Uox$^{-/-}$ rats.

265   According to our previous study, uric acid in wild-type rats' kidney tissue is 174.51 ± 19.61 μg / (g tissue)

266   (Yun et al. 2017). As for the dead offspring, if their uric acid levels in their kidney tissue were much higher

267   than that in wild-type rats, they can also be recognized as likely Uox$^{-/-}$ rats after autopsy. However, only one

268   female rat's likely Uox$^{-/-}$ offspring were obviously healthy. The other two female rats' Uox$^{-/-}$ offspring died

269   several days after birth. Namely, offspring from the third round Uox$^{+/-}$ rats died out, and only offspring from

270   the fourth round Uox$^{+/-}$ rats survived (Table 2). Autopsies of dead rats showed no obvious abnormal organ

271   changes and particularly no visible calculus or sediments were found in kidneys and ureters. The likely Uox$^{-/-}$

272   rats that survived were further identified with molecular biological techniques at enzyme, protein and mRNA

273   levels after their offspring were generated. The identified Uox$^{-/-}$ rats were named "Kunming-DY" rats.

274

275   **Uox$^{-/-}$ rats identification at enzyme level**

276   The increase in A292 was followed by a decreased caused by serum uricase from wild-type rat. As for the

277   reaction system containing Uox$^{-/-}$ rat serum, A292 continuously increased, suggesting there were no uricase

278   activity in Uox$^{-/-}$ rat serum (Fig. 1A). Similar increase was also obtained in liver homogenate from Uox$^{-/-}$ rat

279   (Fig. 1B), though there were differences between serum and liver homogenate in wild-type rat.

280

281   **Uox$^{-/-}$ rats identification by Western blot and RT-PCR**

282   Uox⁻/⁻ rat expresses no normal uricase both at protein levels (Fig. 2A) and mRNA levels (Fig. 2B), while

283   wild-type rat can do so.

284

mRNA mapping

286   The fragments were BLASTed with the mRNA sequence (NM_053768.2), and more than 6000 positive

287   reads were screened out. The results of mRNA mapping based on the positive reads were showed in Fig. 3.

288   The horizontal axis was the reads, and vertical axis showed the sequence of the template mRNA

289   (NM_053768.2). A striped bar means a fragment of a read or the whole read mapped the template mRNA. If

290   there were two or more reads that mapped the same fragment, two or more striped bars were showed behind.

291   The Uox mRNA fragments mapped by reads of wild-type rat almost fully covered the template mRNA (36-

292   1359 nt) (see the vertical axis, Fig. 3A). However, some part (1-35 nt and 71-477 nt) was missing in Uox⁻/⁻

293   rat's mRNA (see the vertical axis, Fig. 3B). After further comparison, it was found that, nucleotide segments

294   from Exon 2, Exon 3 and Exon 4 were completely deleted, and the restored mRNA only contained 917 nt,

295   much shorter than the original one (1359 nt). Therefore, it is impossible for the modified mRNA to translate

296   the right uricase protein.

297

Stable Uox⁻/⁻ rats in general

299   Adult Uox⁻/⁻ rats of the first generation produced by parental Uox⁺/⁻ rats were screened out by SUA and

300   identified by molecular biological techniques. To our surprise, their offspring of the second to the sixth

301   generation were apparently healthy. The numbers of offspring from a couple of parental Uox⁻/⁻ rats varied from

302   6 to 15, and the sex ratio is 0.865 (Male:female = 160:185). When all the offspring were identified as Uox⁻/⁻

303   rats, it can be concluded that their offspring are stable for uricase-deficiency. The survival rate of the five

304   generations (F2-F6) for two months was 99.4% (343/345).The survival rate of the first two generations for one

305   year is 95% in 20 rats (10 male and 10 female), because only one female died of unknown causes. There are no

306   obvious abnormal behaviors without artificial intervention. At the same age, male rats were heavier than the

307   female (Fig. 4A). However, comparing with wild-type SD rats of the same sex, the differences were not

308   significant.

309

SUA, blood fat and serum glucose in stable Uox⁻/⁻ rats

311   The SUA in wild-type rats and heterozygote type rats was under 20 μg/ml in the present study, though the

312   SUA in male rats of wild-type was higher than that in the female (P < 0.05) (Fig 4B). However, the SUA in

313   Uox⁻/⁻ male and female rats (Fig. 4C) were elevated compared to that in wild-type rats (P < 0.05) (See Fig. 4B).

314   Similarly, the SUA in male Uox⁻/⁻ rats (48.4 ± 19.1) was significantly higher than that in females (39.9 ± 20.8)

315   (Fig. 4C) (P < 0.05).

316   Both in wild-type rats and in Uox⁻/⁻ rats, the values of TG, TC, HDL, and LDL were close to or in normal

317   ranges (TG, 0.56-1.7 mmol/l; TC, 3.8-6.1 mmol/l; HDL, 0.78-2.2 mmol/l; and LDL, 2.07-3.1 mmol/l), though

318   the values of TG and LDL in Uox⁻/⁻ rats were significantly different from those in wild-type rats (Fig. 4D).

319   Serum glucose in Uox⁻/⁻ rats was 6.96 ± 1.94 mmol/l (n = 10), also close to the normal range (5.65±1.63

320   mmol/l).

Kidney and its function in Uox⁻/⁻ rats

322   By comparing with wild-type rat kidneys, Uox⁻/⁻ rat kidneys were heavier and larger, but there were no

323   visible spots and other abnormal phenomenon, unlike those damaged by oral adenine (Yun et al. 2016). The

324   LKI of Uox⁻/⁻ rats was significantly bigger than that of wild-type rats (Fig. 5A). The results suggested that renal

325   function of Uox⁻/⁻ rats could be impaired, though there was no other abnormal observation in this visual study.

326   However, the renal function indexes including BUN (Fig 5B) and Cr (Fig. 5C) in Uox⁻/⁻ rats were in or

327   close to normal ranges (BUN, 2.86-7.14 mmol/l; and Cr, 53-106 μmol/l), though BUN in Uox⁻/⁻ rats

328   significantly increased (P < 0.05) while Cr significantly decreased (P < 0.05). Especially, uric acid in Uox⁻/⁻

329   rats' kidney significantly increased (Fig. 5D), which suggested that excessive uric acid was retained in Uox⁻/⁻

330   rats' kidney. However, the differently expressed gene that associated with urate excretion (Lgals9) (Yun et al.

331   2017) and those associated with urate reclamation (Slc22a13 and Slc22a12) (Yun et al. 2017) were down-

332   regulated (Table 3). The differently expressed genes were so insufficient that could not fully explain the

333   retention of uric acid in kidney.

334   The results of histological examination (Fig. 6 and Table 4) showed that slight micromorphological

335   injures occurred in Uox$^{-/-}$ rats. Their glomeruli were enlarged and their capsular spaces were slightly dilated

336   (Fig. 6C). The tubular walls became thin, and the tubular spaces were also slightly dilated (Fig. 6D). Sporadic

337   interstitial fibrosis and inflammatory cell infiltration can also be seen in Uox$^{-/-}$ rat kidneys (Fig. 6C and D). In

338   general, the renal histological changes was mild but with significance (P<0.05) (Table 4).

339

340   **Discussion**

341   Model animals highly mimicking human purine metabolism are necessary for biomedical scientists who

342   study hyperuricemia and associated diseases and for pharmacologists who study uric acid-lowering drugs.

343   Though there are uricase-deficient mice (Lu et al. 2018; Wu et al. 1994), uricase-deficient rats could be a better

344   choice. CRISPR/Cas9 technique (Sapranauskas et al. 2011) is a recent favorite method used most frequently to

345   obtain gene modified animals (Nakamura et al. 2019), but there are often reports of off-target effects (Li et al.

346   2019). Therefore, F0 animals and their offspring should be identified until their stable offspring present

347   expected biological feature. Fortunately, after repeated hybridization and identification, we were able to

348   generate a Uox$^{-/-}$ rat by deleting three exons (from Exon 2 to Exon 4) of the enzyme gene. Unlike Uox$^{-/-}$ mice

349   (Lu et al. 2018; Wu et al. 1994), more than 95% Uox$^{-/-}$ rats are apparently healthy and can survive for more

350   than one year. Like wild-type rats, most parental Uox$^{-/-}$ rats can generate apparently healthy offspring. In honor

351   of Kunming city and its founders, the Uox$^{-/-}$ rat was given the name "Kunming-DY rat".

352   Unlike the SUA levels in Uox$^{-/-}$ mice, the SUA levels in Uox$^{-/-}$ rats were not as high as expected (Lu et al.

353   2018; Wu et al. 1994), although much higher than that in wild-type rats. Mice are small animals, while rats are

354   relative larger than them. Usually, small animals have a much shorter life cycle, meaning that their fast cellular

355   turnover, accompanied with higher metabolic rate, would cause the significant uric acid increase (Liu et al.

356   2019). According to the values tested, the SUA in male Uox$^{-/-}$ rats (48.3 ± 19.1 μg/ml) was proportional to that

357   of men (25-70 μg/ml). In the adult male Uox$^{-/-}$ rats, only a small portion of rats' SUA was above 70 μg/ml. The

358   results suggested that the SUA in all Uox$^{-/-}$ rats is not high enough for a hyperuricemia diagnosis. To establish

359   a "real" hyperuricemia (SUA > 70 μg/ml) model, other treatments, like increasing purine intake or limiting

360   urate excretion, should be added.

361   Fortunately, obvious abnormally functional features, especially obvious disorders of blood fats and serum

362 glucose were not observed in the Uox$^{-/-}$ rats. Though deficiency of uricase can significantly affect TG and LDL

363 levels, the values of all the indexes evaluating blood fat were close to or in the normal ranges. In addition, the

364 values of BUN and Cr, common indexes to evaluate renal function, were also close to or in the normal ranges,

365 though BUN in Uox$^{-/-}$ rats was significantly higher than that in wild-type rats. However, this absence of

366 abnormal function does not mean that uricase-deficiency has no negative impact on rats' renal function.

367 Though the adult Uox$^{-/-}$ rats were apparently healthy, their compensatory renal function was impaired, as

368 demonstrated in the histological examination, which showed slight glomerular and tubular lesion. Considering

369 the rats were able to survive more than one year, the renal injury was much less than that in Uox$^{-/-}$ mice (Lu et

370 al. 2018; Wu et al. 1994). Indeed, the present data suggested that the animal may be vulnerable to substances

371 with renal toxicity, and even more sensitive to factors causing metabolic syndrome. Considering the low

372 survival rate of Uox$^{-/-}$ mice (Lu et al. 2018; Wu et al. 1994) and the high survival rate of large uricase-deficient

373 creatures like humans, elephants and manatees (Sharma & Hiller 2019), uricase may be a key enzyme for small

374 mammal's survival. In addition, compared with the level of SUA in Uox$^{-/-}$ mice, the lower SUA in Uox$^{-/-}$ rats

375 could be associated with urate renal excretion, which needs further investigation.

Conclusions

377   Because Uox$^{-/-}$ rats were uricase-deficient, their purine metabolism, especially their SUA features, is

378 much similar to humans'. In conclusion, the Uox$^{-/-}$ rat is an alternative model animal for studying

379 hyperuricemia and associated disorders, though it needs further investigation to evaluate the animal's other

380 biological features.

381

References

383 Alvarez-Lario B, and Macarron-Vicente J. 2010. Uric acid and evolution. *Rheumatology* 49(11):2010-2015

384 Borghi C, Palazzuoli A, Landolfo M, and Cosentino E. 2019. Hyperuricemia: a novel old disorder-relationship and
385   potential mechanisms in heart failure. *Heart Fail Rev*

386 Chen L, Chen DQ, Wang M, Liu D, Chen H, Dou F, Vaziri ND, and Zhao YY. 2017. Role of RAS/Wnt/beta-catenin
387   axis activation in the pathogenesis of podocyte injury and tubulo-interstitial nephropathy. *Chem Biol*
388   *Interact* 273(56-72

389 Conesa A, Madrigal P, Tarazona S, Gomez-Cabrero D, Cervera A, McPherson A, Szczesniak MW, Gaffney DJ, Elo
390   LL, Zhang X, and Mortazavi A. 2016. A survey of best practices for RNA-seq data analysis. *Genome Biol*
391   17(13

392 Debelle FD, Nortier JL, De Prez EG, Garbar CH, Vienne AR, Salmon IJ, Deschodt-Lanckman MM, and

393   Vanherweghem JL. 2002. Aristolochic acids induce chronic renal failure with interstitial fibrosis in salt-
394   depleted rats. *J Am Soc Nephrol* 13(2):431-436
395 Engel B, Just J, Bleckwenn M, and Weckbecker K. 2017. Treatment Options for Gout. *Dtsch Arztebl Int*
396   114(13):215-222
397 Feig DI. 2014. Serum uric acid and the risk of hypertension and chronic kidney disease. *Curr Opin Rheumatol*
398   26(2):176-185
399 Iwata H, Nishio S, Yokoyama M, Matsumoto A, and Takeuchi M. 1989. Solubility of uric acid and supersaturation
400   of monosodium urate: why is uric acid so highly soluble in urine? *J Urol* 142(4):1095-1098
401 Keebaugh AC, and Thomas JW. 2010. The evolutionary fate of the genes encoding the purine catabolic enzymes in
402   hominoids, birds, and reptiles. *Mol Biol Evol* 27(6):1359-1369
403 Li J, Hong S, Chen W, Zuo E, and Yang H. 2019. Advances in detecting and reducing off-target effects generated
404   by CRISPR-mediated genome editing. *J Genet Genomics*
405 Lin Y, Zhu J, Wang Y, Li Q, and Lin S. 2017. Identification of differentially expressed genes through RNA
406   sequencing in goats (Capra hircus) at different postnatal stages. *PLoS One* 12(8):e0182602
407 Liu D, Yun Y, Yang D, Hu X, Dong X, Zhang N, Zhang L, Yin H, and Duan W. 2019. What Is the Biological
408   Function of Uric Acid? An Antioxidant for Neural Protection or a Biomarker for Cell Death. *Dis Markers*
409   2019(4081962
410 Lu J, Hou X, Yuan X, Cui L, Liu Z, Li X, Ma L, Cheng X, Xin Y, Wang C, Zhang K, Wang X, Ren W, Sun R, Jia Z,
411   Tian Z, Mi QS, and Li C. 2018. Knockout of the urate oxidase gene provides a stable mouse model of
412   hyperuricemia associated with metabolic disorders. *Kidney Int* 93(1):69-80
413 Ma L, Hu J, Li J, Yang Y, Zhang L, Zou L, Gao R, Peng C, Wang Y, Luo T, Xiang X, Qing H, Xiao X, Wu C,
414   Wang Z, He JC, Li Q, and Yang S. 2018. Bisphenol A promotes hyperuricemia via activating xanthine
415   oxidase. *FASEB J* 32(2):1007-1016
416 Mangoff SC, and Milner JA. 1978. Oxonate-induced hyperuricemia and orotic aciduria in mice. *Proc Soc Exp Biol*
417   *Med* 157(1):110-115
418 Nakamura S, Watanabe S, Ando N, Ishihara M, and Sato M. 2019. Transplacental Gene Delivery (TPGD) as a
419   Noninvasive Tool for Fetal Gene Manipulation in Mice. *Int J Mol Sci* 20(23)
420 Ramazzina I, Folli C, Secchi A, Berni R, and Percudani R. 2006. Completing the uric acid degradation pathway
421   through phylogenetic comparison of whole genomes. *Nat Chem Biol* 2(3):144-148
422 Sapranauskas R, Gasiunas G, Fremaux C, Barrangou R, Horvath P, and Siksnys V. 2011. The Streptococcus
423   thermophilus CRISPR/Cas system provides immunity in Escherichia coli. *Nucleic Acids Res* 39(21):9275-
424   9282
425 Schlesinger N. 2017. The safety of treatment options available for gout. *Expert Opin Drug Saf* 16(4):429-436
426 Sharma V, and Hiller M. 2019. Losses of human disease-associated genes in placental mammals. *NAR Genomics*
427   *and Bioinformatics* 2(1)
428 Shen W, Le S, Li Y, and Hu F. 2016. SeqKit: A Cross-Platform and Ultrafast Toolkit for FASTA/Q File
429   Manipulation. *PLoS One* 11(10):e0163962
430 Stavric B, and Nera E. 1978. Use of the uricase-inhibited rat as an animal model in toxicology. *Clin Toxicol*
431   13(1):47-74
432 Trapnell C, Williams BA, Pertea G, Mortazavi A, Kwan G, van Baren MJ, Salzberg SL, Wold BJ, and Pachter L.
433   2010. Transcript assembly and quantification by RNA-Seq reveals unannotated transcripts and isoform
434   switching during cell differentiation. *Nat Biotechnol* 28(5):511-515
435 Wu X, Wakamiya M, Vaishnav S, Geske R, Montgomery C, Jr., Jones P, Bradley A, and Caskey CT. 1994.
436   Hyperuricemia and urate nephropathy in urate oxidase-deficient mice. *Proc Natl Acad Sci U S A* 91(2):742-
437   746
438 Yin H, Hou X, Tao T, Lv X, Zhang L, and Duan W. 2015. Neurite outgrowth resistance to rho kinase inhibitors in
439   PC12 Adh cell. *Cell Biol Int* 39(5):563-576
440 Yun Y, Gao T, Li Y, Gao Z, Duan J, Yin H, and Duan W. 2016. Excretory Function of Intestinal Tract Enhanced in
441   Kidney Impaired Rats Caused by Adenine. *ScientificWorldJournal* 2016(2695718
442 Yun Y, Yin H, Gao Z, Li Y, Gao T, Duan J, Yang R, Dong X, Zhang L, and Duan W. 2017. Intestinal tract is an
443   important organ for lowering serum uric acid in rats. *PLoS One* 12(12):e0190194
444

Figure 1

Uricase activity in serum (A) and liver homogenate (B).

Apart from A292 transiently increasing at the beginning of the reaction, A292 decreased in the reaction system containing serum uricase of wild-type rats. However, A292 continuously increased in the reaction system containing Uox$^{-/-}$ rat serum. The pattern of uricase activity in liver homogenate of Uox$^{-/-}$ rats was similar to that in serum.
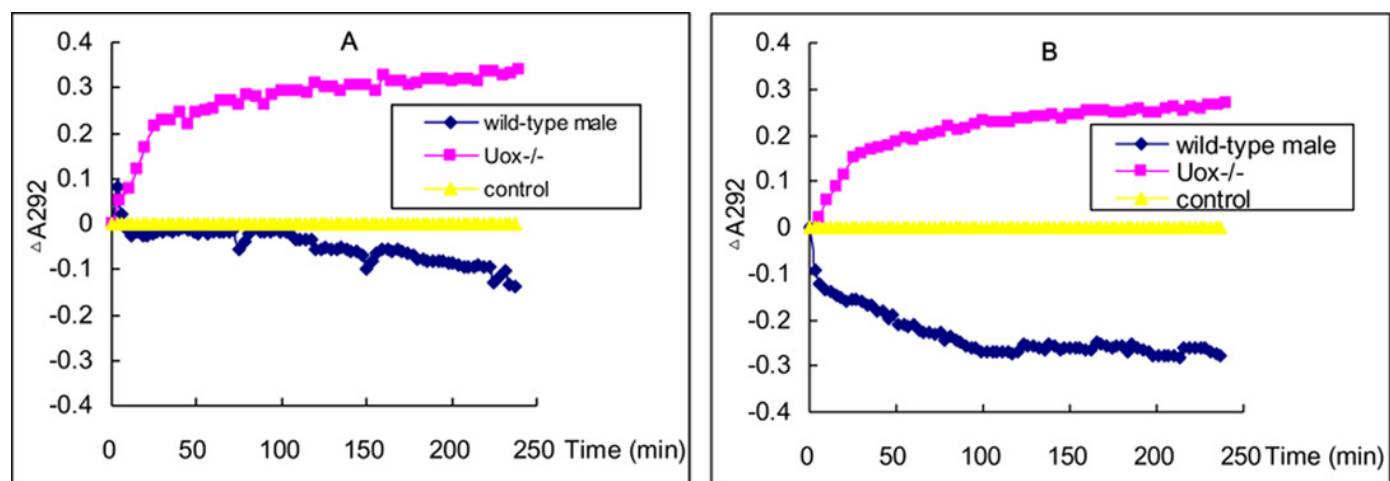
Figure 2

Uricase-deficient rat identified by Western blot (A) and RT-PCR (B).

Uricase protein from wild-type (WT) rat is about 35 kDa and the encoded mRNA results in a

PCR product of about 500 bp. As controls, β-actin (42 kDa) was both positive in Uox^{-/-} and WT

rats, and so was GAPDH (glyceraldehyde 3 phosphate dehydrogenase) (149 bp) in RT-PCR.

However, Uox^{-/-} rats express no normal uricase both at protein level and mRNA level.
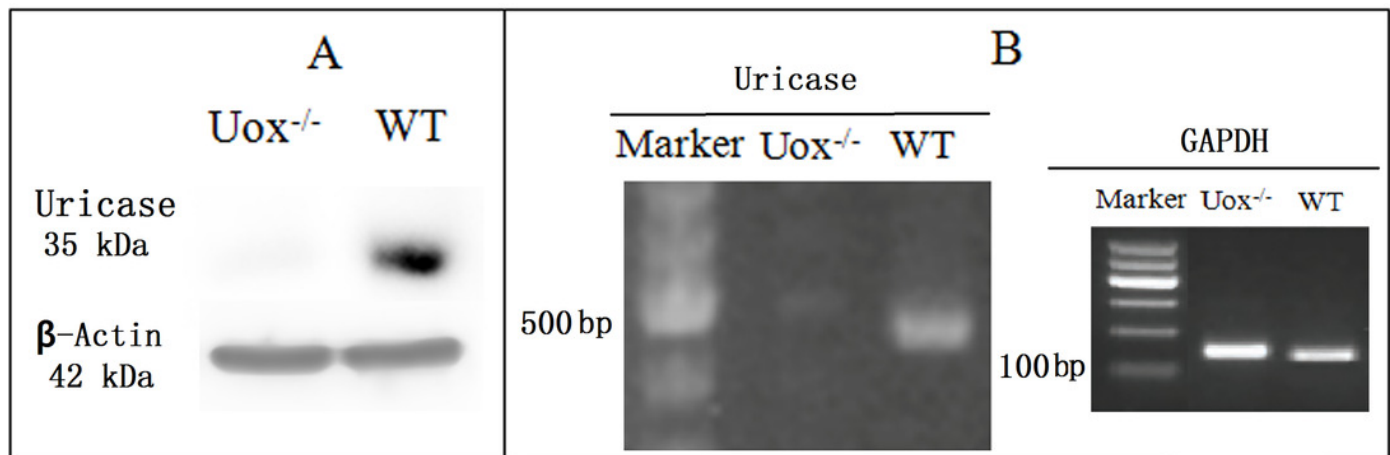
Figure 3

The alignment of RNA-seq reads to the rat Uox mRNA sequence from wild-type (WT) rat (A) and Uox$^{-/-}$ rat (B).

The horizontal axis was the reads, and vertical axis showed the sequence of the template mRNA (NM_053768.2). A striped bar means a fragment mapped by a read or the whole read. If there are two or more reads that mapped the same fragment, two or more striped bars were showed behind. The reads derived from wild-type rat almost fully covered the template mRNA (A). However, the nucleotide segment from Exon 2, 3, and 4 (71-477 nt) was missing in Uox$^{-/-}$ rat (B).
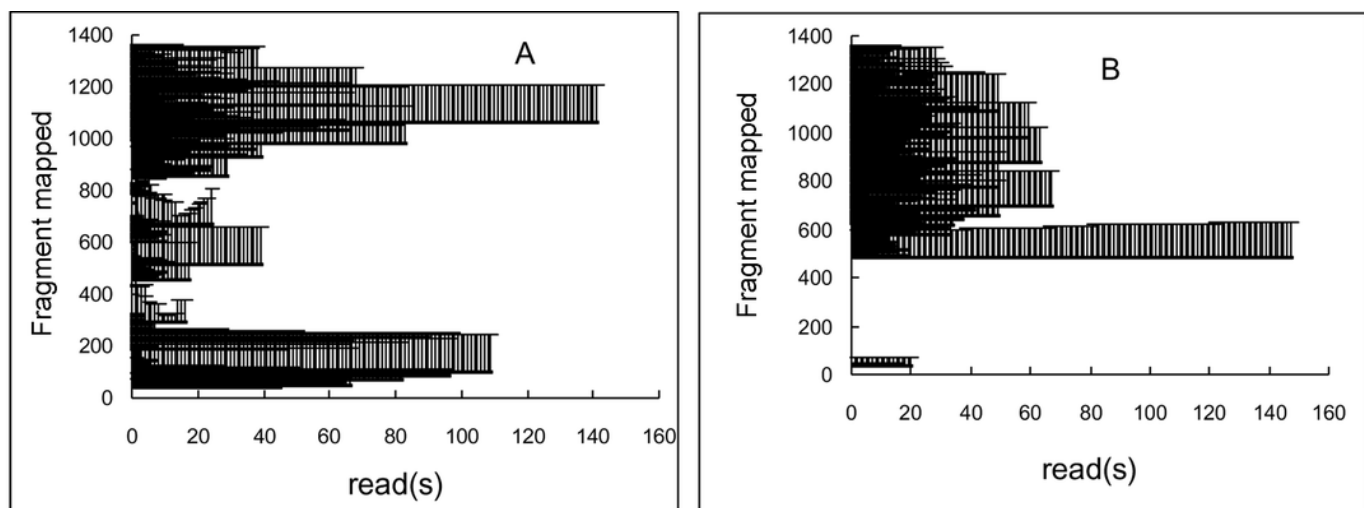
Figure 4

Biological features of Uox$^{-/-}$ rats 45 days after birth (Mean ± SD).

A, Body weight of stable Uox$^{-/-}$ rats (F3, F4, F5 and F6 animal) [n = 160 (male), or 185 (female)]. B, Serum uric acid (SUA) in wild-type rats [n =10 (male), or 9 (female)]. C, SUA in adult Uox$^{-/-}$ rats (F3, F4, F5 and F6 animal) [n = 160 (male), or 185 (female)]. D, Blood fat in wild type rats [n = 20 (10 male, 10 female)] and in Uox$^{-/-}$ rats [n = 12 (7 male, 5 female)]. * P < 0.05, independent Student's t-test (two tailed). TG, total triglyceride; TC, total cholesterol; HDL, high density lipoprotein; LDL, low density lipoprotein.
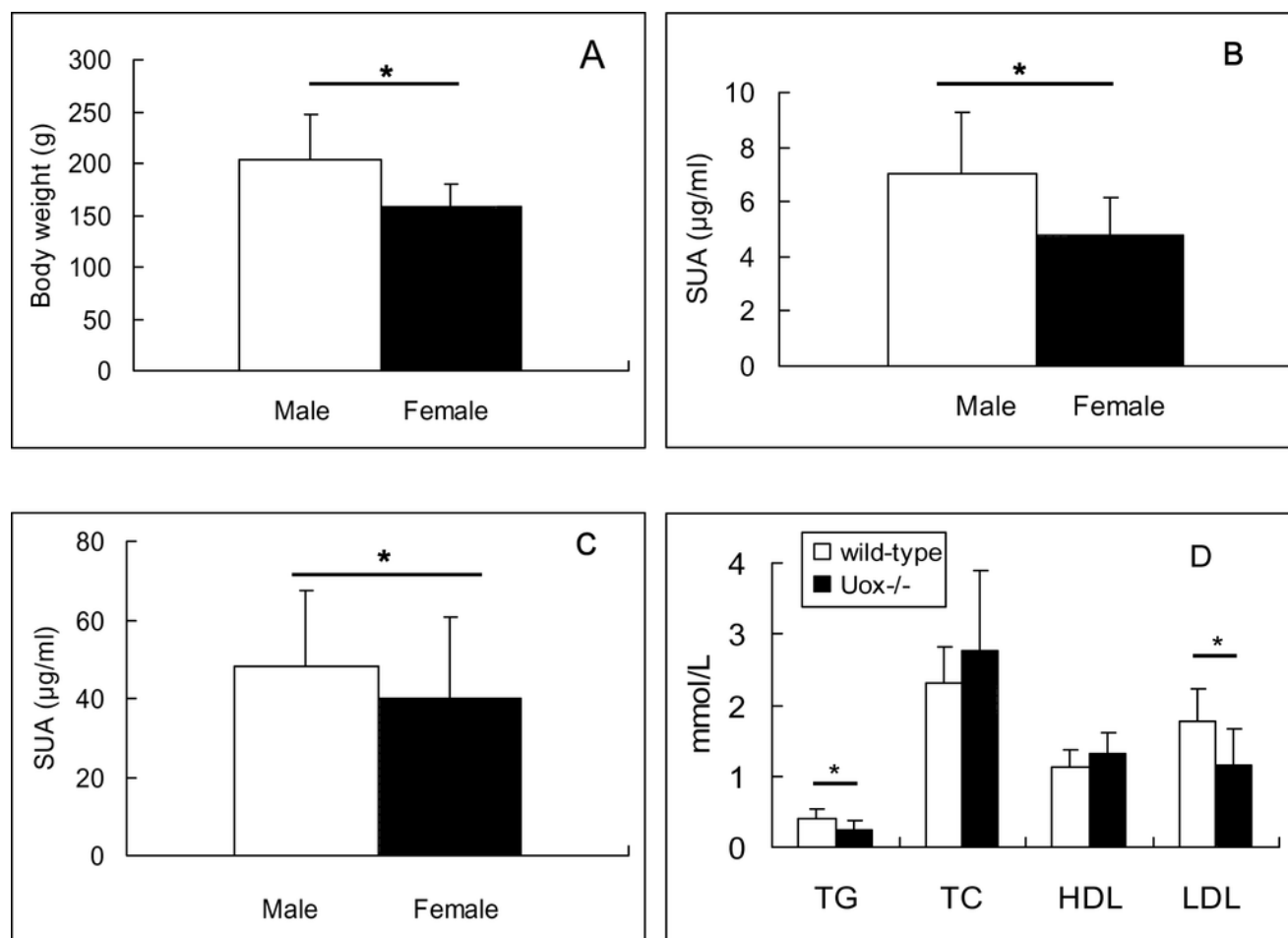
Figure 5

Kidney of male Uox$^{-/-}$ rats and its function (Mean ± SD).

Left kidney index (LKI) in Uox$^{-/-}$ rats (n = 7) was bigger that that in wild-type rats (n = 10) (A).

BUN in Uox$^{-/-}$ rats (n = 10) was higher than that in wild-type rats (n = 5) (B). However, Cr in

Uox$^{-/-}$ rats (n = 10) was lower than that in wild-type rats (n = 5) (C). Uric acid in Uox$^{-/-}$ rats'

kidney (n = 9) was higher than that in male wild-type rats' (n = 8) (D). BUN, blood urea

nitrogen; Cr, serum creatinine. * P < 0.05, independent Student's t-test (two tailed)
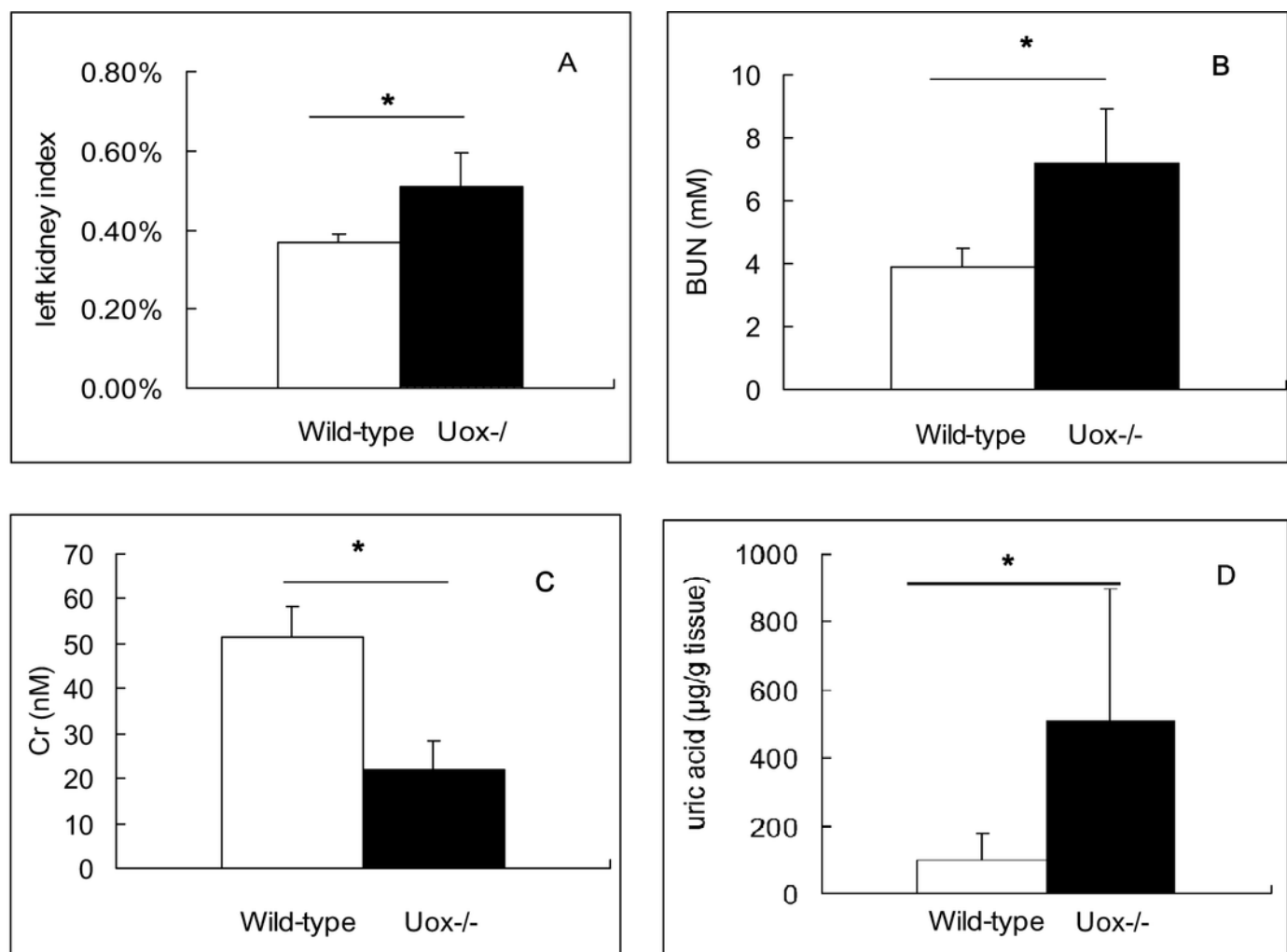
Figure 6

Microscopic histology of rat kidneys in male wild-type rats (A, B) and Uox$^{-/-}$ rats (C, D).

Nephrocytes in wild-type rats were piled tightly (A, B); and there were no swelling signs in glomeruli (A) and tubules (B). Meanwhile in Uox$^{-/-}$ rats, cells in the glomeruli were slightly swollen and their capsular spaces were slightly dilated (C), the tubular walls became thin, and their spaces were also slightly dilated (D). Sporadic interstitial fibrosis and inflammatory cell infiltration can also be seen in the kidneys of Uox$^{-/-}$ rats (C, D). Bar = 50 μm
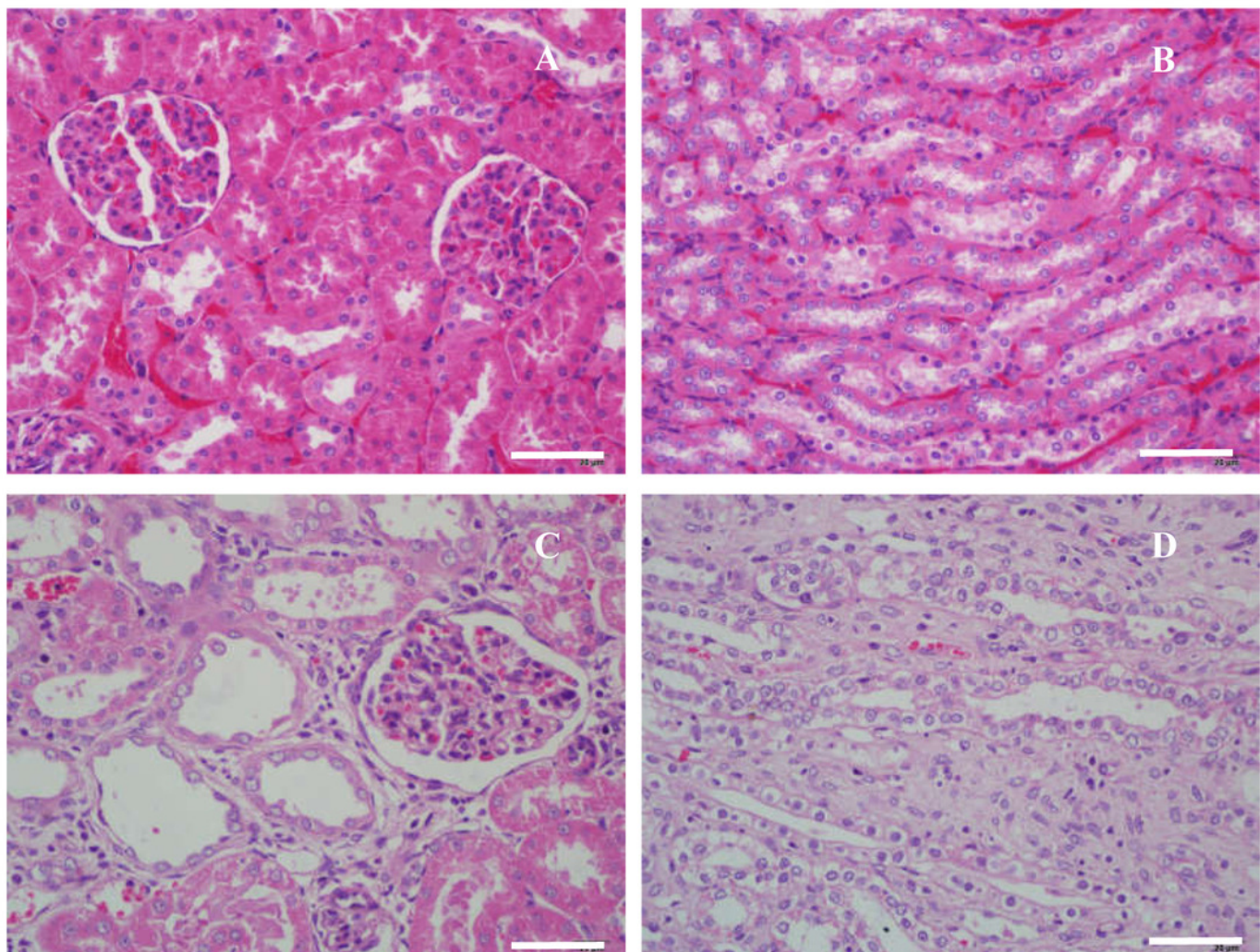
SUA (μg/ml) of adult $Uox^{+/-}$ rat.

No.	gender	Serum uric acid (SUA)	Mean ± SD	note
1	Male	20.91		Third round
2	Male	9.92	13.80±6.17	Third round
3	Male	10.57		Fourth round
4	Female	13.78		Third round
5	Female	19.00	17.03±2.84	Fourth round
6	Female	18.31		Fourth round

Likely Uox$^{-/-}$ rats screened out from F0 offspring*

a Male rats with SUA above 40 μg/ml or female rats with SUA above 30 μg/ml were

recognized as likely Uox$^{-/-}$ rats. b Likely Uox$^{-/-}$ rats died several days after birth. The dead rats were identified based on the uric acid in their kidney above 1000 μg/(g tissue). * The number of offspring (F1) was 6 (3/3, male/female), the number of F2 animal was 48 (22/26), the number of F3 animal was 105 [47/(58-1)], the number of F4 animal was 47 [(14-1)/33], the number of F5 animal was 70 (36/34), and the number of F6 animal was 75 (41/34).

Cage	Offspring (Male/Female)	[a,] Likely Uox$^{-/-}$ rats (Male/Female)	other rats (Male/Female)	Note
1	9 (4/5)	7 (2/5), died [b]	2 (2/0)	From third round Uox$^{+/-}$ rats
2	3 (2/1)	3 (2/1), died [b]	0	From third Uox$^{+/-}$ rats
3	14 (8/6)	6 (3/3)	8 (5/3)	From fourth Uox$^{+/-}$ rats

Genes associated with uric acid transport or metabolism expressed in male rat kidneys (mean ± SD, n = 3).

FPKM, Fragment Per Kilobases of exon model per Million mapped reads. * P<0.05,

independent Student's t-test, two-tailed. # the expression of Uox in Uox$^{-/-}$ rat is invalidated.

No	Gene	FPKM		P	Fold(b/a)	Alias	Note
		a wild-type	b Uox$^{-/-}$	(a vs b)			
1	Abcg2	71.19±10.03	79.90±8.91	0.324	1.12	BCRP1	secretion
2	Abcc4	17.17±2.02	13.89±1.17	0.072	0.81	MRP4	secretion
3	Lgals9	13.62±2.34	7.40±1.77	0.021*	0.54	UAT	secretion
4	Slc17a1	44.01±4.75	54.49±6.00	0.077	1.24	NPT1	secretion
5	Slc22a6	541.93±36.04	505.83±51.18	0.374	0.93	OA1	secretion
6	Slc2a9	7.21±0.36	7.62±0.37	0.237	1.06	GLUT9	reclamation
7	Slc2a6	1.03±0.057	0.88±0.094	0.076	0.85	GLUT9	reclamation
8	Slc22a13	11.67±3.25	3.42±0.05	0.012*	0.29	OAT10	reclamation
9	Slc22a8	395.78±47.31	433.38±31.86	0.317	1.10	OAT3	reclamation
10	Slc22a12	396.99±33.77	285.08±43.38	0.024*	0.72	URAT1	reclamation
11	Xdh	35.45±3.79	37.95±3.84	0.467	1.07	UOR	synthesis
12	Uox$^{\#}$	0.03±0.06	0.01±0.01	0.507	0.25	UOX	degradation
13	Ada	9.59±2.00	8.01±1.62	0.347	0.84	ADA	synthesis

Scores of renal microscopic pathology (n = 3).

*Mann-Whitney U model (two tailed)

Item	Wild-type			Uox^{-/-}		
	Sample1	Sample2	Sample3	Sample1	Sample2	Sample3
Glomerular abnormality	0	0	0	1	1	1
Tubular atrophy	0	0	0	1	1	1
Tubular necrosis	0	0	0	1	1	1
Lymphocytic infiltrates	0	0	0	1	1	1
Interstitial fibrosis	0	1	0	1	1	1
sum	0	1	0	5	5	5
P*				0.034		